Transactions of the **14th International Conference on Structural Mechanics in Reactor Technology** (SMiRT 14), Lyon, France, August 17-22, 1997

G06/5

Stress intensity factors for elbows with axial surface crack at crown

Viswanatha N., Bhate S.R., Kushwaha H.S.
Bhabha Atomic Research Centre, India

ABSTRACT :

In the structural integrity assessment, stress intensity factor(SIF) for a given crack geometry is an important input for prediction of fatigue crack propagation and crack stability. Elbows are highly stressed components in piping system. Fracture mechanics analysis of the elbow with an axial internal surface crack at crown is carried out using finite element technique. The SIF distributions for short and long elbow with varying crack aspect ratio and wall thickness are presented. The result of elbow under internal pressure are compared with cylinder solution.

1. INTRODUCTION :

The analysis of surface flaws in pressurised shells in nuclear power plants, is important for the structural integrity assessment. Linear Elastic Fracture Mechanics (LEFM) methodology has been applied successfully for studying the fatigue crack growth and life estimation. The fatigue crack growth predictions are based on stress intensity factor (SIF) range and fatigue resistance of the material. SIF can also be used for estimating crack stability under elastoplastic stress state by simplified methods such as R6 method. Hence determination of SIF is of great importance in the component life estimation and margin assessment the failure.

Elbows are important part of the piping system. Their dimensions are governed by the layout of the piping and other design requirements of the system. Because of their lower stiffness in comparison to straight pipes, they help to reduce the thermal forces and moments within a system by undergoing deformation. Under inplane bending load, Cesari et al [5] observed that the circumferential stress component is maximum near the crown and the sign of the stress is dependent on whether opening or closing moment is applied. Diem et al [7] and Doi et al [8] carried out extensive experimental study on elbows. The location of maximum stress was found at crown irrespective of the bend angle of elbow[7]. For the closing moment, the stresses are tensile on inner surface and hence surface cracks were found to grow after large number of load cycles. Apart from this, the internal pressure acting on the elbow will result in circumferential stress which will try to open the crack. Hence in the fracture study of the elbow neighborhood of crown position is a critical location. However, very few studies with crack at crown have been reported and they are concerned with through wall crack.

In some limiting situations, approximation based on plate or cylinder may be employed for obtaining the SIF. But a general surface flaw must be treated as three dimensional problem because of the complexity of crack geometry and the stress distribution around flaw. In components like elbows and tees in nuclear reactor, the stresses are induced by pressure, temperature and seismic loading. In such situations, simplification may lead to large inaccuracy. Sauter et al [15] analysed right angled elbow with surface crack at crown by Continuum approach and Line Spring method. Uhlmann et al [16] studied the elbow with combined load of internal pressure and bending moment, using 3D finite elements.

2. Analysis method:

Though 3D fracture mechanics problem is solved by various numerical methods such as finite element method, boundary integral equations, boundary element method, weight function approach, the finite element approach has been extensively used because of its flexibility and availability of versatile packages. The influence coefficients for different type of stress distributions can be obtained by 3D FEA and used for the given type of stress distribution to obtain the SIF [12]. For calculating fracture parameters, 3D finite element analyses are prohibitively costly and time consuming. Therefore, engineer looks for an economical method with adequate accuracy. The line spring model offers an economic tool in estimating crack loading in surface cracked shells. Rice and Levy [13,14] introduced the concept of line spring by approximating 3D crack analysis as a quasi 2D shell problem. This method is becoming more popular for its simplicity in modeling surface crack and computational economy with adequate accuracy. SIF and J-integral values obtained by this method by Sauter [15] are within 10% accuracy when compared to 3D analysis. Erdogan [9] has used this method for studying surface cracks on extrados and intrados considering both longitudinal and circumferential orientation of the crack.

In the Line spring model, the cracked continuum is replaced by continuously distributed Single edge crack (SEC) notched specimens along the crack front. The stiffness of ligament is defined by continuously distributed spring elements connecting the two free faces of the fictitious through crack. The stiffness of spring at any location relates generalised stress and moment resultants to cracked displacements and rotations in a single edge-cracked plate with same crack depth. The solution of plate/shell or continuum with distributed stiffness leads to displacements and force distribution. The crack force intensity at any location is derived from single edge cracked plate subjected to the tension and bending moments. Rice [13] used line spring with plate elements. Ritchie et al [6] extended line spring for use with isoparametric brick elements.

In the present study an opening moment and internal pressure loading are considered on axial crown crack on inner surface. The aspect ratio (2c/a) chosen is 5 and 10. The crack depth ratio (a/t) are taken as 0.2, 0.5 and 0.8. The elbow parameters considered are elbow curvature (R/r_m) as 1.5 and 3 and shell parameter (r_m/t) 4.5 and 10.5. For the case of straight pipe, the empirical solution for these crack geometry and shell parameter are obtained by Raju -Newman [12]. The elbow curvature considered covers considerable range of bends used in the piping system. Fig. 1 shows schematically the elbow with postulated flaw. The geometric parameters of the crack considered are also illustrated in the Figure 1.

3. Results and Discussion :

The elbow is modeled using shell elements (S8R) and the surface crack is modeled using line spring elements (LS6) available in ABAQUS [1] element library. Half of the elbow is modeled using the symmetry condition on the mid plane. To simulate realistic constraints imposed by connecting piping, straight pipe of six times the mean radius of the elbow is connected to free end of elbow. The axial forces are acting on free end of the elbow when under internal pressure and in second case bending moment is applied at the free end. The mesh has 340 elements and 8450 degrees of freedom. The mesh is validated by comparing the results of J-integral values under inplane bending moment of 1.1 MN-m on a elbow with published ones [15]. The calculated J-integral values are compared with reported values as shown in the Fig.2. Other parameters like deflection under the load and the crack driving force distribution also show close agreement. The line spring element is known to predict poor results near the end of crack where crack meets free surface due to corner singularity weaker than square root singularity assumed in single edge cracked plate in line spring formulation [3,4,11]. Hence in the present work, the results near the free surface are not presented.

The loading considered are internal pressure and opening mode bending moment. The closing bending moment causes compressive hoop stress at crown on inner surface of the bend hence crack closure is expected on inner surface. Therefore it need not be separately considered. The crack face pressure is taken into consideration in the case of internal pressure. In both the cases, variation of mode I SIF is studied. The SIF is normalised by $\sigma\ (\pi a/Q)^{0.5}$ where σ is hoop stress for internal pressure (pr_m/t) and bending stress ($M/\pi r_m^2 t$) in case of bending load and Q is the shape factor for the elliptical crack ($Q=1+1.464(a/c)^{1.65}$).

Fig. 3 shows the Mode I SIF distribution for an elbow of r_m/t =10.5 and R/r_m=1.5 the crack aspect ratio (2c/a) considered is 5. The crack depth ratios (a/t) considered are 0.2, 0.5 and 0.8. The corresponding cylinder SIF are also shown in Fig. 3. It can be seen that there is significant increase in the SIF for the elbow compared to that of a cylinder with same r_m/t ratio.

For the same elbow under in-plane bending moment, the SIF distribution is shown Fig.4. The SIF distribution is showing a different trend for the bending load. With the increase in crack depth (deep crack sizes), the SIF values are found to decrease towards the point of maximum depth. The point of maximum SIF is shifting towards region where the crack meets the surface. The stress distribution across the thickness of elbow studied explains this behavior. The stress distribution under some conditions, is known to cause even negative SIF [9]. Under opening moment, circumferential stress distribution across the thickness at the crown changes its sign. Hence the stress acting on the crack front at deeper locations is lesser than the stresses at farther point. Thus SIF, being function of local stress distribution, changes accordingly. This change in SIF pattern allows the growth of crack then along the length direction. This is also observed in the fatigue experiments where the shallow cracks propagates in depth direction initially and then propagation continues along the length [7, 15].

Table 1 gives normalised SIF for short elbow (R/r_m=1.5) under internal pressure and external bending moment. The. normalised SIF is given at four angular positions. The cylinder ratios (r_m/t) considered are 4.5 and 10.5 which cover the elbows present in main Primary Heat Transport (PHT) piping of 500 MW(e) PHWR. Table 2 gives corresponding results for long elbow.

The elbow correction factors ($F_{elbow}/F_{cylinder}$) for internal pressure case are given in Table 3 and 4 at different angular locations of the crack for short and long elbow. This is multiplication factor to Raju-Newman [12] cylinder solution for the axial cracks in cylinder.

From Tables 3 and 4, the maximum correction factor of 1.2651 is to be applied for short elbow with long crack (2c/a= 10) and depth ratio(a/t) of 0.2. For cracks on a thick elbow (r_m/t=4.5), the elbow solution is close to that given by the cylinder solution. At deepest point of the crack, SIF is higher than the cylinder solution for all the elbows considered for the study except for short elbow (R/r_m =1.5) with crack aspect ratio (2c/a) of 10 and crack depth ratio (a/t) of 0.8. At deepest location, the variation of elbow correction factor are given in Fig. 5 and 6. It is seen that for thick elbows the solution approaches the cylinder solution. It is seen that for highly curved (R/r_m =1.5) thick elbow, SIF is slightly less than the cylinder solution. This behavior is due to finite accuracy of LSM. This type of small differences can be observed in results by Erdogan [9] also.

The study of effect of elbow curvature on the SIF is made as a special case and the convergence of elbow SIF distribution with cylinder solution by increasing the bend radius is shown in Fig. 7. The crack depth ratio considered (a/t) is 0.8 and crack aspect ratio(2c/a) taken is 5. The elbow solution gradually approaches the cylinder solution with increase in the bend radius (R).

4. CONCLUSIONS :

In the present work elbow with internal surface crack on the crown is analysed under internal pressure and in-plane bending moment. The crack driving force variation along the crack front is studied for two different bend radius (R/r_m) of 1.5 ,3 and r_m/t of 4.5and 10.5. The crack aspect ratio (2c/a) studied are 5 and 10. The crack depths considered are 20, 50 and 80% the wall thickness.

The SIF distribution for elbow under internal pressure is considerably higher than that of a straight pipe (having same dimensions of pipe and crack), is more for thinner pipe and shallow cracks. The location of maximum depth on crack front is region of peak SIF in case of internal pressure. However in case of bending moment load, peak SIF occurs away from the point of maximum crack depth. The elbow curvature correction factor is higher for short radius elbows and decreases with increase either in the bend radius or thickness or crack depth of the elbow. For thick elbows the present work predicts the SIF close to that of straight pipe. For determining SIF at free surface detailed 3D analysis is essential.

REFERENCES :

1. ABAQUS Version 5.3 Hibbit, Karlson and Associates, 1992.
2. ASME Boiler and Pressure Vessel Code, Section XI, 1992
3. Benthem. J.P, 'State of stress at the Vertex of a quarter-infinite crack in half space', Int. Journal of Solids and structures, Volume 13, 1977, pp.479-492.
4. Bazant. Z.P and Estensorro. L.F ' Surface singularity and crack propagation' Int. Journal of Solids and structures, Volume 15, 1979, pp.405-426.
5. Cesari F.G. et al 'In-plane bending test piping elbow', Nuclear Engineering and Design, Volume 116, 1989, pp. 215-221.
6. David Ritchie et al 'The Application of Line Spring Fracture Mechanics Methods to Design of complex welded structures', American Society for Testing and Materials, STP 1131, 1992, pp. 113-131.
7. Diem .H et al 'Failure Behavior of Thick Walled, Austenitic pipe bends under Cyclic Bending Loading at Constant Internal Pressure' Nuclear Engineering and Design, Volume 151, 1994, pp.269-289.
8. Doi et al 'Structural analysis of elbow with Surface crack', The 1990 Pressure vessel and piping conference, Nashville, Tennessee, June 17-21, 1990, PVP-195, ASME, pp. 99-104.
9 Erdogan. F et al 'Surface Cracks in Toroidal Shells', Transactions of XII conference on Structural Mechanics in Reactor Technology, Volume G, paper 06/1, 1993, pp. 81-86.
10. Muller K.U. et al ' Deformation Behavior of Elbows', Transactions of VIII conference on Structural Mechanics in Reactor Technology, Volume F, Paper 7/9, 1985
11. Nakamura. T and Parks. D. M ' Three-dimensional Stress Field near the crack front of a thin elastic plate', Journal of Applied Mechanics, ASME, Volume 55, 1988, pp. 805-813.
12. Raju. I.S. et al 'Stress Intensity Factors for internal and external Surface Cracks in Cylindrical Shells' Journal of Pressure Vessel Technology, Volume 104, 1982, pp. 293-298.

13. Rice. J.R. and Levy. N ' The Part Through Surface Crack in Elastic Plate', ASME, Journal of Applied Mechanics, Volume 39, 1972, pp. 185-194.
14. Rice J.R. and Levy. N. 'The Line Spring for Surface Flaws: in :The Surface Crack: Physical Problems and Computational Solutions', ed. Swedlow. J.L., American Society of Mechanical Engineers, 1972.
15. Sauter. A et al 'Fracture Mechanics Analysis of a Pipe Elbow', Nuclear Engineering and Design, Volume 112, 1989, pp. 211-220.
16. Uhlmann. D et al 'Fracture Mechanics study of a pipe bend with a longitudinal crack under static loading', Nuclear Engineering and Design, Volume 119, 1990, pp. 347-360.

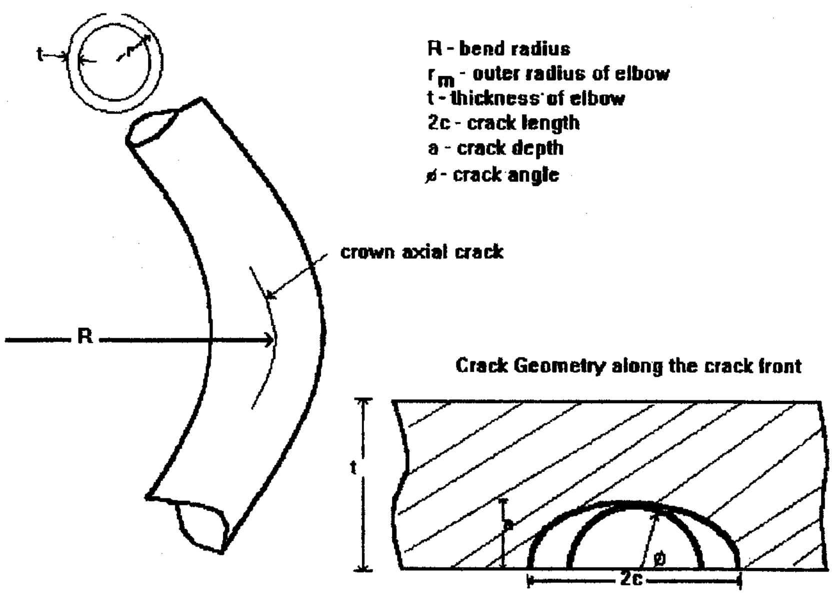

Figure 1 Elbow with internal axial crack on crown

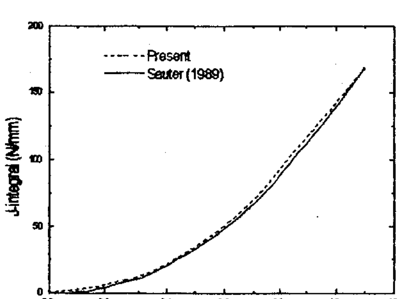

FIG. 2 Validation Test on Model

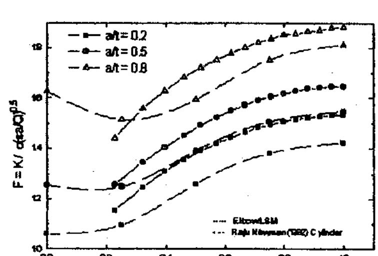

FIG. 3 Normalised SIF Distribution $R/r_m = 1.5$, $r_m/t = 4.5$, $2c/a = 5$ (Internal Pressure)

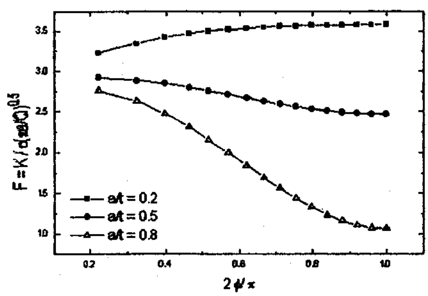

FIG. 8 Normalised SIF Distribution Rb/t=3, r/t =10.5, 2c/a=5
(Bending Moment)

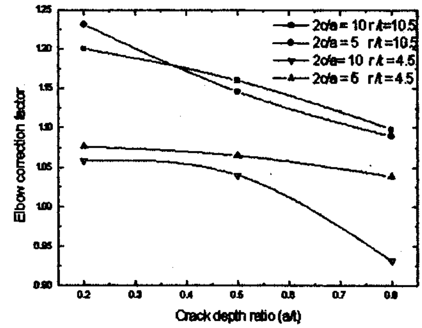

Fig. 5 Elbow correction Factor for short elbow (R/r_m = 1.5)

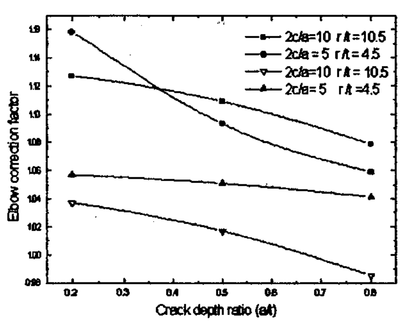

Fig. 6 Elbow correction factor for long elbow (R/r_m = 3)

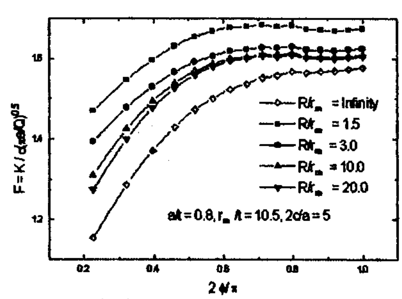

FIG. 7 Effect of curvature on SIF Distribution
(Internal Pressure)

Table. 1 Normalised SIF for Short elbow (R/r_m= 1.5)

		2c/a= 10						2c/a=5					
		Internal Pressure a/t			Bending moment a/t			Internal pressure a/t			Bending moment a/t		
r_m/t	$2\phi/\pi$	0.2	0.5	0.8	0.2	0.5	0.8	0.2	0.5	0.8	0.2	0.5	0.8
10.5	0.25	1.073	1.277	1.675	4.121	4.207	4.534	1.193	1.269	1.490	4.488	4.125	3.910
	0.50	1.339	1.588	2.078	4.869	4.558	4.526	1.370	1.428	1.648	4.886	3.980	3.269
	0.75	1.477	1.791	2.236	5.170	4.620	3.850	1.469	1.528	1.681	5.019	3.738	2.312
	1.0	1.524	1.857	2.279	5.261	4.602	3.422	1.502	1.561	1.674	5.040	3.612	1.818
4.5	0.25	1.073	1.245	1.419	2.178	2.094	2.011	1.176	1.279	1.473	2.395	2.178	2.034
	0.50	1.355	1.596	1.8727	2.587	2.363	2.158	1.379	1.479	1.709	2.632	2.165	1.819
	0.75	1.512	1.826	2.181	2.774	2.451	2.033	1.494	1.606	1.834	2.727	2.072	1.447
	1.0	1.565	1.905	2.328	2.830	2.470	1.942	1.533	1.648	1.884	2.754	2.021	1.245

Table. 2 Normalised SIF for long elbow (R/r_m= 3.0)

		2c/a= 10						2c/a=5					
		Internal Pressure a/t			Bending moment a/t			Internal pressure a/t			Bending moment a/t		
r_m/t	$2\phi/\pi$	0.2	0.5	0.8	0.2	0.5	0.8	0.2	0.5	0.8	0.2	0.5	0.8
10.5	0.25	1.002	1.211	1.638	3.009	3.0196	3.271	1.114	1.188	1.414	3.257	2.913	2.728
	0.50	1.249	1.513	2.030	3.484	3.222	3.177	1.288	1.353	1.585	3.488	2.767	2.202
	0.75	1.387	1.711	2.195	3.683	3.218	2.596	1.361	1.455	1.626	3.561	2.566	1.448
	1.0	1.431	1.776	2.239	3.744	3.185	2.024	1.413	1.490	1.628	3.577	2.468	1.066
4.5	0.25	1.054	1.257	1.538	1.605	1.588	1.647	1.145	1.259	1.496	1.721	1.583	1.505
	0.50	1.331	1.606	2.003	1.897	1.752	1.688	1.354	1.464	1.730	1.918	1.552	1.291
	0.75	1.483	1.826	2.310	2.023	1.778	1.517	1.466	1.585	1.844	1.982	1.463	0.959
	1.0	1.535	1.905	2.452	2.058	1.177	1.416	1.505	1.627	1.889	2.00	1.420	0.800

Table 3. Elbow correction factor for short elbow (R/r_m=1.5)

		2c/a= 10			2c/a=5		
		Internal Pressure a/t			Internal pressure a/t		
r_m/t	$2\phi/\pi$	0.2	0.5	0.8	0.2	0.5	0.8
10.5	0.25	1.2651	1.2058	1.1577	1.2858	1.1791	1.137
	0.50	1.2463	1.184	1.1852	1.2765	1.1772	1.1891
	0.75	1.2077	1.664	1.1188	1.2423	1.1542	1.119
	1.00	1.2003	1.1594	1.0980	1.2309	1.1453	1.089
4.5	0.25	1.0641	1.0029	0.8995	1.0728	1.0247	0.972
	0.50	1.0662	1.0319	0.9350	1.0947	1.0631	1.0716
	0.75	1.0583	1.0389	0.9289	1.081	1.0656	1.0467
	1.0	1.0576	1.0395	0.9320	1.0763	1.0645	1.0386

Table 4. Elbow correction factor for long elbow (R/r_m=3)

		2c/a= 10			2c/a=5		
		Internal Pressure a/t			Internal pressure a/t		
r_m/t	$2\phi/\pi$	0.2	0.5	0.8	0.2	0.5	0.8
10.5	0.25	1.1813	1.1433	1.1322	1.2006	1.1041	1.0793
	0.50	1.1626	1.1281	1.1578	1.2001	1.1152	1.1436
	0.75	1.1342	1.1143	1.0983	1.1511	1.0992	1.0822
	1.00	1.1271	1.1089	1.0787	1.158	1.0931	1.0592
4.5	0.25	1.0451	1.0121	0.9210	1.0446	1.0087	0.9876
	0.50	1.0474	1.0384	0.9991	1.0752	1.0523	1.0851
	0.75	1.0383	1.0389	0.9830	1.0601	1.0516	1.0523
	1.0	1.0371	1.0395	0.9851	1.0568	1.0512	1.0413